Photochemical & Photobiological Sciences

PAPER

View Article Online
View Journal | View Issue

Cite this: *Photochem. Photobiol. Sci.*, 2015, **14**, 982

Quantitative assessment of photostability and photostabilisation of Fluvoxamine and its design for actinometry

Mounir Maafi* and Wassila Maafi

Received 16th January 2015,
Accepted 8th March 2015

DOI: 10.1039/c5pp00022j

www.rsc.org/pps

Despite the numerous concerns that have been raised in relation to considering 0th, 1st and 2nd-order kinetic treatments for photodegradation characterisation and assessment of drugs, they still are employed, as they are the only tools available for these types of studies. The recently developed Φ-order kinetic models have opened new perspectives in the treatment of photoreaction kinetics and stand as the best known alternative to the classical approach. The Φ-order kinetics have been applied here to Fluvoxamine (Fluvo) with the aim of setting out a detailed and comprehensive procedure capable of rationalising photodegradation/photostability of drugs and proposing a platform for photosafety studies. Our results prove that quantum yields of drugs ($0.0016 < \Phi^{\lambda_{irr}}_{Fluvo} < 0.43$) should *a priori* be considered wavelength-dependent; their photostabilisation (up to 75% for Fluvo) by means of absorption competitors can explicitly be related to a decrease of the photokinetic factor, and photoreversible drugs can be developed into efficient actinometers (as Fluvoxamine in the 260–290 nm range). A pseudo-rate-constant factor was proposed as a descriptive parameter, circumventing the limitations of overall rate-constants and allowing a comparison between kinetic data of drugs obtained under different conditions.

1. Introduction

A vast number of drugs have been shown to be adversely affected by light both *in vivo* and *in vitro*.[1–4] Consequently, several studies have been devoted to the elucidation of the mechanisms, photo-products, kinetics and photoprotection strategies of such photodegradation reactions.[5–7] Thus far, the kinetic analysis of these reactions has relied solely on the classical thermal zeroth-, first- and second-order reaction models.[5,6] Nevertheless, despite the fact that it soon became evident that such treatment strategies are not suited for photochemical reactions, they continued to be employed, mainly due to the lack of more adequate alternative treatments, procedures and methods. This situation has considerably limited the scope and reliability of drug photodegradation and photostabilisation studies. The efforts that may have been devoted to proposing integrated rate-laws for photokinetic data that truly reflect the evolution of photoreactions are very scarce in the literature and predominantly based on approximations. This *status quo* is due to the tedious and mostly unsolvable mathematical hurdles encountered during integration of photoreactions' differential equations.[8,9] Recently, an approach was proposed whereby semi-empirical rate-law model equations could be developed for photodegradation reactions. It has also been shown that such photoreactions obeyed a Φ-order kinetics, with a quite different formulation than the classical ones.[10,11] The Φ-order kinetic models, which proved to successfully describe photoreactions of drugs undergoing unimolecular or reversible isomerization,[10,12] have considerably facilitated photostability investigations.

Fluvo is a selective serotonin (5-hydroxytryptamine, 5-HT) neuronal re-uptake inhibitor (SSRI) used in the treatment of depression and anxiety.[13–15] It has a few side effects[16] and little or no anticholinergic effect which makes it a much less hazardous drug than other antidepressants especially in overdose quantities.[17,18]

While this molecule is stable under hydrolysis,[19] it undergoes reversible geometric photoisomerism under UV irradiation around the oxime linker group, Scheme 1.[20] The occurrence of only one photoproduct (*Z*-Fluvo) was evidenced

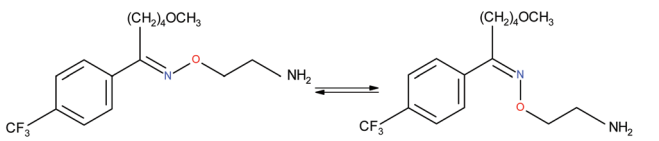

Scheme 1 *E*/*Z* (*anti*/*syn*) reversible photoisomerism of Fluvo upon exposure to UV-irradiation.

Leicester School of Pharmacy, De Montfort University, The Gateway, Leicester LE1 9BH, UK. E-mail: mmaafi@dmu.ac.uk

for the photodegradation of *E*-Fluvo.[20,21] While a number of pharmacological experiments have failed to link the *Z*-isomer to any phototoxicity, it was nonetheless found to be a 150-times less potent than its *E*-counterpart when tested on cortical synaptosomes.[19,22] UVB irradiation was deemed responsible for *E*-Fluvo isomerisation and thus interaction of this type of radiation with Fluvo and subsequent isomerisation could occur even *in vivo* since UVB is able to reach blood vessels in the dermis.[20] Incidentally, the occurrence of SSRIs in aquatic environments, wastewater and even drinking water sources has also been reported.[23] As such, the study of the photodegradation kinetics of these drugs becomes important not only from a pharmacological but also from an environmental point of view.

Very little is known on the photodegradation kinetics of Fluvo.[20,21] Its photodegradation was attributed the pseudo-first order kinetics under fluorescent lamp irradiation (with a beam bandwidth of 110 nm, ranging between 290–400 nm with a maximum emission at 312 nm)[21] and differing half-life times were recorded depending on the spectral output of the lamps used for irradiation.[20] Relatively low quantum yield values of Fluvo photodegradation in different aqueous media (1.87×10^{-3} to 8.55×10^{-3}) have been recorded for the experiment using irradiation light from fluorescent lamps.[21] Nevertheless, to the best of our knowledge, neither quantum yield determination for the individual forward ($E \rightarrow Z$) and reverse ($Z \rightarrow E$) reactions nor experiments involving UVB radiation have, thus far, been attempted.

In this paper, the issues highlighted above have been addressed together with a quantification of the effect of light absorbing competitors and Fluvo suitability for actinometry.

2. Materials and methods

2.1 Materials

Fluvoxamine maleate, 2-{[(*E*)-{5-methoxy-1-[4-(trifluoromethyl)-phenyl]pentylidene}amino]oxy}ethanamine (*E*-Fluvo), glacial acetic acid and spectrophotometric grade acetonitrile were purchased from Sigma-Aldrich. Double distilled water was used as the solvent.

2.2 Monochromatic continuous irradiation

For irradiation experiments, a Ushio 1000 W xenon arc-lamp light source housed in a housing shell model A6000 and powered by a power supply model LPS-1200, was used. This set up was cooled by tap water circulation through a pipe system. The lamp housing was connected to a monochromator model 101 that allows the selection of specific irradiation wavelengths since it consists of a special f/2.5 monochromator with a 1200 groove per mm at 300 nm blaze grating. The excitation beam was guided through an optical fibre to impinge from the top of the sample cuvette *i.e.* the excitation and the analysis light beams were perpendicular to each other. The set up (lamp, lamp housing and monochromator) was manufactured by Photon Technology International Corporation.

2.3 The monitoring system

A diode array spectrophotometer (Agilent 8453) was used to measure the various absorption spectra and kinetic profiles for the irradiation and calibration experiments. This spectrophotometer was equipped with a 1 cm cuvette sample holder and a Peltier system model Agilent 8453 for temperature control. As such, the sample was kept at 22 °C, stirred continuously during the experiment, and completely shielded from ambient light. The spectrophotometer was monitored by an Agilent 8453 Chemstation kinetics software.

A radiant power/energy meter model 70260 was used to measure the radiant power of the incident excitation beams.

2.4 Kinetic data treatment

In order to carry out non-linear fittings and to determine best-fit curves, a Levenberg–Marquardt iterative program within the Origin 6.0 software was used.

2.5 HPLC measurements

The HPLC system consisted of a reversed-phase Jupiter 5μ C-18 300A Phenomenex (250 × 4.60 mm) column equipped with a Perkin Elmer Series 200 pump, UV/Vis detector, vacuum degasser and a Perkin Elmer type Chromatography Interface 600 series Link linked to a computer system.

The mobile phase consisted of 60% double distilled water adjusted to pH 4.8 with glacial acetic acid and 40% acetonitrile. A flow rate of 1.5 ml min^{-1} and an injection loop of 20 μl were used. The detector wavelength was set at 245 nm. Retention times of 10 and 8.32 min were recorded for *E* and *Z* isomers, respectively.

2.6 Fluvo solutions

A 2.88×10^{-4} M stock solution of Fluvo in water was prepared by weighing the solid. The flask was protected from light by aluminium foil wrapping and was kept in the fridge. The stock solution was diluted to prepare fresh analytical solutions (*ca.* 2×10^{-6} M) for analysis of irradiation experiments performed at various wavelengths.

For actinometric studies, Fluvo solutions of the same concentrations (*ca.* 2.9×10^{-6} M) were exposed to specific irradiation wavelengths (260, 270, 280, 285 and 290 nm) using a series of different intensities for each wavelength. The kinetic traces were observed at the observation wavelength λ_{obs} = 245 nm and subsequently fitted with the Φ-order equations.

Experiments were conducted at least in triplicates.

3. Results and discussion

3.1 The mathematical background

3.1.1 Φ-Order kinetics for non-isosbestic irradiation. The kinetic data of direct unimolecular photoreactions and photoreversible dimolecular phototransformations, collected at non-isosbestic and monochromatic irradiation at constant temperature, have recently been shown to obey Φ-order

kinetics.[8,10–12] Φ-order kinetics is much more suitable to describe photoreactions than the classical treatments proposed for zeroth-, first- and second-order thermal reactions. Even though ubiquitous, the treatment of photokinetics on the basis of the latter classical reaction orders is unreliable, for at least three main drawbacks inherently linked to this approach. Firstly, the differential equations of photoreactions are generally different from and not possibly integrated in closed-forms as is the case for thermal reactions of 0^{th}-, 1^{st}- or 2^{nd}-order. This means that using such classical order treatments for the quantitative investigation of photoreactions must be considered as a mere approximation. Secondly, literature data have reported that the classical approach may lead to a confusion about the reaction order that should be attributed to the photodegradation reaction at hand given that the kinetic data of a given reaction (generally up to half-life time) can well be fitted by the equations corresponding to two different reaction orders (most commonly 0^{th}- and 1^{st}-order). Thirdly, the rate-constant values determined from the experimental data of photodegradation cannot be analytically linked to the experimental conditions and/or reaction attributes. This has made it difficult to compare such rate constants between compounds and/or laboratories.

In this context, the approach adopted to develop the equations of Φ-order kinetics offers a more robust mathematical framework to investigate photoreactions. The model equation, a logarithmic expression involving a time-dependent exponential term, for unimolecular photoreactions where only the initial species absorbs, has been derived through closed-form integration.[8] This model equation represents the basis for the development of the semi-empirical model equations for both the unimolecular photoreaction where both initial species and photoproducts absorb, and photoreversible reactions. They have been optimised by studying simulated photoreaction traces obtained by numerical Runge–Kutta integration methods.[10,11] These traces, calculated for a wide range of experimental conditions for unimolecular[10] and reversible photoreactions,[11] served for referencing the reliability and validation of the proposed semi-empirical integrated rate-laws.

A unique set of general equations (eqn (1a) and (1b)) can be derived for photochemical reactions involving two species, the initial molecule, A, and its photoproduct, B, whose transformations might be achieved by one A → B or two (A ⇌ B) photochemical steps, each one characterised by a specific photoreaction quantum yield (Φ_{AB} and Φ_{BA}). Such systems are labelled as AB(1Φ) and AB(2Φ), respectively. Hence, if it is assumed that the concentration of the excited state is negligible during the progress of the photoreaction while the reaction medium is concomitantly maintained at a constant temperature, homogeneously stirred, and continuously irradiated with a monochromatic beam (with the latter beam's non-isosbestic wavelength (λ_{irr}) corresponding to a spectral region where species A and B absorb different amounts of light (P) *i.e.*, the absorption coefficients (ε) of the species are different and might have non-zero values $\left(\varepsilon_A^{\lambda_{irr}} \neq \varepsilon_B^{\lambda_{irr}} \neq 0\right)$, then under these conditions, the concentration profiles, $C_A(t)$ and $C_B(t)$, are dependent on the species absorption coefficients, and given by (eqn (1a) and (1b)) where $k_{A\rightleftharpoons B}^{\lambda_{irr}}$ is the overall reaction rate-constant, and $l_{\lambda_{irr}}$ is the optical path length of the excitation light across the reactive medium.

For spectrophotometric monitoring of the reaction's evolution, it is preferable to use the logarithmic integrated rate-law equation describing the variation of the total observed absorption $\left(A_{tot}^{\lambda_{irr}/\lambda_{obs}}(t)\right)$ with time, eqn (2).[11] It involves only the cumulative observed absorbances $\left(A_{tot}^{\lambda_{irr}/\lambda_{obs}}\right)$ of the medium which have been measured under the observation ($l_{\lambda_{obs}}$) and not the excitation ($l_{\lambda_{irr}}$) condition (with $l_{\lambda_{obs}}$ being the optical path length of the monitoring light inside the sample). These optical path lengths ($l_{\lambda_{irr}}$ and $l_{\lambda_{obs}}$) are not necessarily equal for a given experiment, and the absorbance of the medium under the excitation conditions (*i.e.* corresponding to a measurement along $l_{\lambda_{irr}}$) may not be directly accessible during the experiment.

The coefficients $A_{tot}^{\lambda_{irr}/\lambda_{obs}}(t)$, $A_{tot}^{\lambda_{irr}/\lambda_{obs}}(0)$, $A_{tot}^{\lambda_{irr}/\lambda_{obs}}(\mathrm{pss})$, $A_{tot}^{\lambda_{irr}/\lambda_{irr}}(0)$ and $A_{tot}^{\lambda_{irr}/\lambda_{irr}}(\mathrm{pss})$ in eqn (2) are the measured (along $l_{\lambda_{obs}}$) total absorbances of the medium respectively recorded at reaction time t, at the initial time ($t = 0$) and either at the end of the reaction or at the photostationary state (pss, where $t = \infty$). The reaction medium is irradiated at a given irradiation wavelength and simultaneously monitored at either a different observation wavelength ($\lambda_{irr}/\lambda_{obs}$) or at the same wavelength

$$C_A(t) = C_A(\infty) + \frac{\log\left[1 + \left(10^{\left[\left(\varepsilon_A^{\lambda_{irr}} - \varepsilon_B^{\lambda_{irr}}\right) \times (C_A(0) - C_A(\infty)) \times l_{\lambda_{irr}}\right]} - 1\right) \times e^{-k_{A\rightleftharpoons B}^{\lambda_{irr}} \times t}\right]}{\left(\varepsilon_A^{\lambda_{irr}} - \varepsilon_B^{\lambda_{irr}}\right) \times l_{\lambda_{irr}}} \quad (1a)$$

$$C_B(t) = C_B(\infty) \times \left(1 - \frac{\log\left[1 + \left(10^{\left[\left(\varepsilon_A^{\lambda_{irr}} - \varepsilon_B^{\lambda_{irr}}\right) \times (C_A(0) - C_A(\infty)) \times l_{\lambda_{irr}}\right]} - 1\right) \times e^{-k_{A\rightleftharpoons B}^{\lambda_{irr}} \times t}\right]}{\left(\varepsilon_A^{\lambda_{irr}} - \varepsilon_B^{\lambda_{irr}}\right) \times (C_A(0) - C_A(\infty)) \times l_{\lambda_{irr}}}\right) \quad (1b)$$

$$A_{tot}^{\lambda_{irr}/\lambda_{obs}}(t) = A_{tot}^{\lambda_{irr}/\lambda_{obs}}(\infty) + \frac{A_A^{\lambda_{irr}/\lambda_{obs}}(0) - A_{tot}^{\lambda_{irr}/\lambda_{obs}}(\infty)}{A_A^{\lambda_{irr}/\lambda_{irr}}(0) - A_{tot}^{\lambda_{irr}/\lambda_{irr}}(\infty)} \times \frac{l_{\lambda_{obs}}}{l_{\lambda_{irr}}} \log\left[1 + \left(10^{\left[\left(A_A^{\lambda_{irr}/\lambda_{irr}}(0) - A_{tot}^{\lambda_{irr}/\lambda_{irr}}(\infty)\right) \times \frac{l_{\lambda_{irr}}}{l_{\lambda_{obs}}}\right]} - 1\right) \times e^{-k_{A\rightleftharpoons B}^{\lambda_{irr}} \times t}\right] \quad (2)$$

($\lambda_{irr}/\lambda_{irr}$). It is assumed that the reaction is quantitative and proceeds without by-products.

The analytical expression of the exponential factor, $k^{\lambda_{irr}}_{A\rightleftharpoons B}$, in eqn(1) and (2) which represents the overall reaction rate-constant, is given by,[11]

$$k^{\lambda_{irr}}_{A\rightleftharpoons B} = \left(\Phi^{\lambda_{irr}}_{A\rightarrow B}\times\varepsilon^{\lambda_{irr}}_{A} + \Phi^{\lambda_{irr}}_{B\rightarrow A}\times\varepsilon^{\lambda_{irr}}_{B}\right)\times l_{\lambda_{irr}}\times F_{\lambda_{irr}}(\infty)\times P_{\lambda_{irr}} = \beta_{\lambda_{irr}}\times P_{\lambda_{irr}} \quad (3)$$

where $\Phi^{\lambda_{irr}}_{A\rightarrow B}$ and $\Phi^{\lambda_{irr}}_{B\rightarrow A}$ are the forward and reverse quantum yields of the reaction photochemical steps realised at the irradiation wavelength (λ_{irr}); $P_{\lambda_{irr}}$ is the radiant power (expressed in einstein dm^{-3} s^{-1}); $\beta_{\lambda_{irr}}$ is a proportionality factor, and $F_{\lambda_{irr}}(\infty)$ the time-independent photokinetic factor expressed as:

$$F_{\lambda_{irr}}(\infty) = \frac{1-10^{-\left(A^{\lambda_{irr}/\lambda_{irr}}_{tot}(\infty)\times\frac{l_{\lambda_{irr}}}{l_{\lambda_{obs}}}\right)}}{A^{\lambda_{irr}/\lambda_{irr}}_{tot}(\infty)\times\frac{l_{\lambda_{irr}}}{l_{\lambda_{obs}}}} \quad (4)$$

As it has been previously shown,[11] eqn (2) describing the kinetics of AB(2Φ) systems, can also allow to retrieve the equations set out for pure unimolecular AB(1Φ) reactions ($\Phi^{\lambda_{irr}}_{B\rightarrow A}=0$), where either (i) only the initial compound absorbs the irradiation light (under these conditions $A^{\lambda_{irr}/\lambda_{obs}}_{tot}(\infty)=0$ and $F_{\lambda_{irr}}(\infty)$ = 2.3 $\cong$ Ln(10))[8,24] or (ii) both the initial compound and its photoproduct (A and B) absorb light at the irradiation wavelength (which corresponds to the complete depletion of species A, and therefore, $F_{\lambda_{irr}}(\infty)$ is calculated using eqn (4) with $A^{\lambda_{irr}/\lambda_{irr}}_{tot}(\infty)=A^{\lambda_{irr}/\lambda_{irr}}_{B}(\infty)=\varepsilon^{\lambda_{irr}}_{B}\times l_{\lambda_{irr}}\times C_A(0)$).[10]

The differentiation of eqn (2) yields the expression of the initial velocity of the reaction $\left((dA_{tot}/dt)_{t=0}=v^{\lambda_{irr}/\lambda_{obs}}_{0(mod.)}\right)$, for the kinetic trace involving the variation of the total absorbance,[11]

$$v^{\lambda_{irr}/\lambda_{obs}}_{0(mod.)} = \left(\frac{dA^{\lambda_{irr}/\lambda_{obs}}_{tot}}{dt}\right)_0 = \frac{A^{\lambda_{irr}/\lambda_{obs}}_{tot}(0)-A^{\lambda_{irr}/\lambda_{obs}}_{tot}(pss)}{A^{\lambda_{irr}/\lambda_{irr}}_{tot}(0)-A^{\lambda_{irr}/\lambda_{irr}}_{tot}(pss)}\times\frac{k^{\lambda_{irr}}_{A\rightleftharpoons B(mod.)}}{\frac{l_{\lambda_{irr}}}{l_{\lambda_{obs}}}\times Ln(10)} \times\left(10^{\left(A^{\lambda_{irr}/\lambda_{irr}}_{tot}(pss)-A^{\lambda_{irr}/\lambda_{irr}}_{tot}(0)\right)\times\frac{l_{\lambda_{irr}}}{l_{\lambda_{obs}}}}-1\right) \quad (5)$$

The numerical value of eqn (5), obtained graphically, corresponds to the theoretical expression derived from the differentiation of the reaction,[11] as

$$v^{\lambda_{irr}/\lambda_{obs}}_{0(cld.)} = \left(\varepsilon^{\lambda_{obs}}_{B}-\varepsilon^{\lambda_{obs}}_{A}\right)\times l_{\lambda_{obs}}\times\Phi^{\lambda_{irr}}_{A\rightarrow B}\times\varepsilon^{\lambda_{irr}}_{A}\times l_{\lambda_{irr}}\times F_{\lambda_{irr}}(0)\times C_0\times P_{\lambda_{irr}} = \delta_{\lambda_{irr}}\times P_{\lambda_{irr}} \quad (6)$$

When calculating $v^{\lambda_{irr}/\lambda_{obs}}_{0(cld.)}$, the photokinetic factor $F_{\lambda_{irr}}(t)$ at time t = 0 takes the value of $F_{\lambda_{irr}}(0)$, that is determined using $A^{\lambda_{irr}/\lambda_{irr}}_{tot}(0)=\varepsilon^{\lambda_{irr}}_{A}\times l_{\lambda_{irr}}\times C_A(0)$ in lieu of $A^{\lambda_{irr}/\lambda_{irr}}_{tot}(\infty)$ in eqn (4). $\delta_{\lambda_{irr}}$ is a proportionality factor.

Because eqn (1) and (2) are semi-empirical, their application has been limited to $F_{\lambda_{irr}}(\infty)$ values higher than 1.2. This condition is easily met by reducing the values of either the initial concentration of species A or the optical path length for irradiation, $l_{\lambda_{irr}}$.[10,11]

3.1.2 Isosbestic irradiation equations. In the case where monochromatic irradiation of the solution is realised at an isosbestic point, λ_{irr} = λ_{isos} (only a few isosbestic points are usually present on the electronic spectra of AB(2Φ) reactions), the general integrated rate-law of AB reaction systems has been obtained through a closed-form integration,[25] as

$$C_A(t) = C_A(\infty)+(C_A(0)-C_A(\infty))\times e^{-k^{\lambda_{isos}}_{A\rightleftharpoons B}\times t} \quad (7)$$

$$C_B(t) = C_B(\infty)-C_B(\infty)\times e^{-k^{\lambda_{isos}}_{A\rightleftharpoons B}\times t} \quad (8)$$

with $C_A(\infty)$ and $C_B(\infty)$, the concentrations of the species at either the end of the reaction or pss ($t=\infty$) and $k^{\lambda_{isos}}_{A\rightleftharpoons B}$, the overall rate-constant of the reaction performed at isosbestic irradiation.

$k^{\lambda_{isos}}_{A\rightleftharpoons B}$ has the same analytical expression as eqn (3) but with λ_{isos} replacing λ_{irr} and the photokinetic factor $F_{\lambda_{isos}}$ used instead of $F_{\lambda_{irr}}(\infty)$. $F_{\lambda_{isos}}$ is calculated using eqn (4) with $A^{\lambda_{isos}/\lambda_{isos}}_{tot}$ instead of $A^{\lambda_{irr}/\lambda_{irr}}_{tot}(\infty)$.

The value of the initial velocity can be obtained graphically and compared to its theoretical expression (eqn (9)).

$$v^{\lambda_{isos}/\lambda_{isos}}_{0} = -k^{\lambda_{isos}}_{A\rightleftharpoons B}\times(C_A(0)-C_A(pss)) = -\Phi^{\lambda_{isos}}_{A\rightarrow B}\times C_A(0)\times\varepsilon^{\lambda_{isos}}_{A}\times l_{\lambda_{isos}}\times P_{\lambda_{isos}}\times F_{\lambda_{isos}} \quad (9)$$

The monoexponential form of eqn (7) and (8) indicates that isosbestic irradiation induces first-order kinetics for AB(2Φ) reactions. This is primarily due to the fact that when λ_{irr} = λ_{isos}, the photokinetic factor does not vary with reaction time (as the medium absorbance at the irradiation wavelength, λ_{isos}, is time-independent).

3.1.3 The kinetic elucidation method for AB(2Φ) photoreversible reactions. If, *a priori*, we suppose that the quantum yields of the photoreaction are wavelength-dependent (until proven otherwise) and the spectra of the species A and B overlap, then the equations set out above for both isosbestic (eqn (7) and (8)) and non-isosbestic (eqn (1) and (2)) irradiations can fit well the AB(2Φ) experimental traces obtained photometrically, however, the extracted fitting parameters ($k^{\lambda_{isos}}_{A\rightleftharpoons B}$ and $v^{\lambda_{isos}/\lambda_{obs}}_{0}$ or $k^{\lambda_{irr}}_{A\rightleftharpoons B}$ and $v^{\lambda_{irr}/\lambda_{obs}}_{0}$), which represent two equations for each irradiation condition, are not sufficient to work out the three unknowns of the reaction namely, its photochemical quantum yield values and the absorption coefficient, $\varepsilon^{\lambda_{irr}}_{B}$ (*i.e.* the electronic spectrum) of the photoproduct, if none of the latter is available prior to the experiment. Solving the kinetics by using only the fitting parameters (irrespective of the number of $\lambda_{irr}/\lambda_{obs}$ traces) leads to a

degenerate kinetic solution with inextricable identifiability and/or distinguishability issues.[26]

In order to overcome this situation, we have recently proposed a simple elucidation method for photoreversible reactions that can be implemented in three steps.[26]

Firstly, the reaction quantum yields are determined for an isosbestic irradiation. The variation of the species concentrations during photodegradation, under monochromatic irradiation at an isosbestic point, is monitored by HPLC. At a given irradiation wavelength (λ_{iso}), the absorption coefficient of the photoproduct is known ($\varepsilon_A^{\lambda_{iso}} = \varepsilon_B^{\lambda_{iso}}$) and therefore, the number of unknowns is only two ($\Phi_{A\to B}^{\lambda_{iso}}$ and $\Phi_{B\to A}^{\lambda_{iso}}$) for this experiment.

Hence, fitting the experimental data with eqn (7) and (8) provides the numerical values for the reaction initial velocity ($v_0^{\lambda_{iso}}$, eqn (9)) and the reaction overall rate-constant $\left(k_{A\rightleftharpoons B}^{\lambda_{iso}}\right)$. Under these conditions, solving the system of two equations ($v_0^{\lambda_{iso}}$ and $k_{A\rightleftharpoons B}^{\lambda_{iso}}$), leads to the determination of the absolute values of $\Phi_{A\to B}^{\lambda_{iso}}$ (eqn (10)) and $\Phi_{B\to A}^{\lambda_{iso}}$ (eqn (11)), as

$$\Phi_{A\to B}^{\lambda_{iso}} = \frac{k_{A\rightleftharpoons B}^{\lambda_{iso}}}{\varepsilon_A^{\lambda_{iso}} \times l_{\lambda_{iso}} \times P_{\lambda_{iso}} \times F_{\lambda_{iso}}} \times \frac{(C_A(0) - C_A(\text{pss}))}{C_A(0)} \quad (10)$$

$$\Phi_{B\to A}^{\lambda_{iso}} = \frac{k_{A\rightleftharpoons B}^{\lambda_{iso}}}{\varepsilon_A^{\lambda_{iso}} \times l_{\lambda_{iso}} \times P_{\lambda_{iso}} \times F_{\lambda_{iso}}} - \Phi_{A\to B}^{\lambda_{iso}} \quad (11)$$

Both the species pss concentrations and the quantum yield values allow determining the equilibrium constant (eqn (12)),

$$K_{\rightleftharpoons}^{\lambda_{iso}} = \frac{k_{B\to A}^{\lambda_{iso}}}{k_{A\to B}^{\lambda_{iso}}} = \frac{C_B(\text{pss})}{C_A(\text{pss})} = \frac{\Phi_{A\to B}^{\lambda_{iso}}}{\Phi_{B\to A}^{\lambda_{iso}}} \quad (12)$$

It is worth noting that $K_{\rightleftharpoons}^{\lambda_{iso}}$ is concentration-independent. This feature finds its importance in the fact that the HPLC experiment that served its determination is usually performed at initial concentrations of species A that are not suitable (too concentrated) for spectrophotometric analyses (which are bound to be realised at lower concentrations, specifically, where $F_{\lambda_{irr}}(\infty) > 1.2$ as discussed above).

The reconstruction of the full spectrum of the photoisomer (B), can then be performed at lower concentrations in the second step of the elucidation method. This is achieved from the value of $K_{\rightleftharpoons}^{\lambda_{iso}}$ and the spectrum of the reactive medium recorded at pss under the same isosbestic irradiation used for the HPLC experiment $\left(A_{tot}^{\lambda_{iso}/\lambda_{obs}}(\text{pss})\right)$, as

$$\varepsilon_B^{\lambda_{obs}} = \frac{(K_{\rightleftharpoons}^{\lambda_{iso}} + 1) \times A_{tot}^{\lambda_{iso}/\lambda_{obs}}(\text{pss}) - \varepsilon_A^{\lambda_{obs}} \times l_{\lambda_{obs}} \times C_A(0)}{l_{\lambda_{obs}} \times K_{\rightleftharpoons}^{\lambda_{iso}} \times C_A(0)} \quad (13)$$

Therefore, irrespective of the wavelength selected to perform the irradiation, the number of unknowns will constantly be two in total, as the spectrum of the photoproduct (ε_B^{λ}) is fully known.

Hence, in the last step of the method, the quantum yields for each non-isosbestic irradiation wavelength ($\Phi_{A\to B}^{\lambda_{irr}}$ and $\Phi_{B\to A}^{\lambda_{irr}}$) can readily be worked out by using eqn (6) and its numerical value given by eqn (5) (for $\Phi_{A\to B}^{\lambda_{irr}}$, eqn (14)) and by rearranging eqn (3) (for $\Phi_{B\to A}^{\lambda_{irr}}$) to give eqn (15).

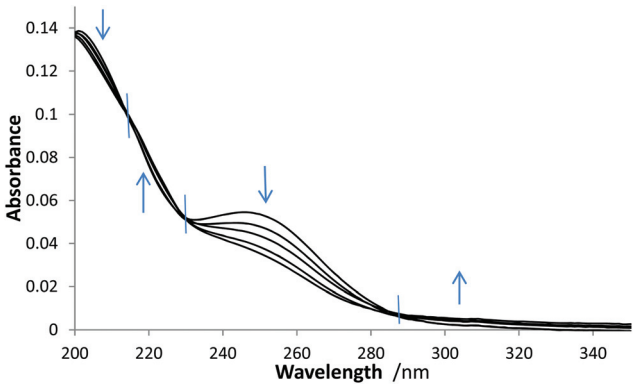

Fig. 1 Evolution of the electronic absorption spectra of 4.01×10^{-6} M Fluvo in water subjected to steady state irradiation with a 270 nm monochromatic beam (total irradiation time 26 min at a radiant power of 7.37×10^{-7} einstein s^{-1} dm^{-3}). The arrows indicate the direction of the absorbance evolution during the photoreaction and the vertical lines cross the spectra at the isosbestic points (215, 226, 285 nm).

$$\Phi_{A\to B}^{\lambda_{irr}} = \frac{v_{0(\text{mod.})}^{\lambda_{irr}/\lambda_{obs}}}{\left(\varepsilon_B^{\lambda_{obs}} - \varepsilon_A^{\lambda_{obs}}\right) \times l_{\lambda_{obs}} \times \varepsilon_A^{\lambda_{irr}} \times l_{\lambda_{irr}} \times P_{\lambda_{irr}} \times F_{\lambda_{irr}}^0 \times C_A(0)} \quad (14)$$

$$\Phi_{B\to A}^{\lambda_{irr}} = \frac{k_{A\rightleftharpoons B}^{\lambda_{irr}}}{\varepsilon_A^{\lambda_{irr}} \times l_{\lambda_{irr}} \times P_{\lambda_{irr}} \times F_{\lambda_{irr}}(\infty)} - \Phi_{A\to B}^{\lambda_{irr}} \quad (15)$$

3.2 Fluvo photoreaction

The native electronic absorption spectrum of *E*-Fluvo isomer (Fig. 1) can be divided into two main absorption regions, 200–226 nm ($\log(\varepsilon) = 4.5$) and 226–320 nm ($\log(\varepsilon) = 4.1$). This molecule, thus, absorbs mainly in the UVB region of the spec-

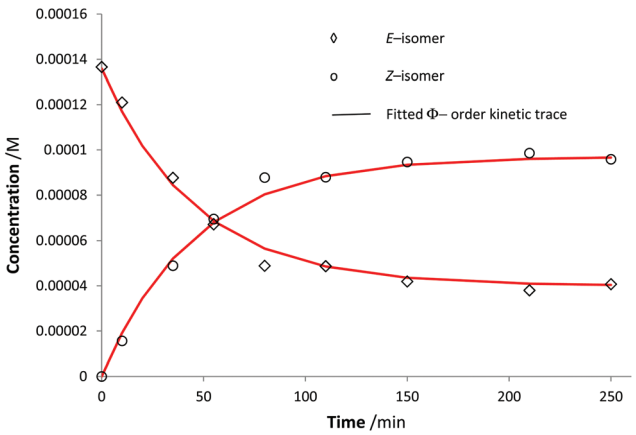

Fig. 2 Change in aqueous *E*-Fluvo solution (1.37×10^{-4} M) and its *Z*-isomer photoproduct concentrations over 4 hours upon exposure to an isosbestic monochromatic irradiation of 226 nm ($P_{226} = 1.88 \times 10^{-6}$ einstein s^{-1} dm^{-3}) as monitored by HPLC.

Table 1 Overall rate-constant and equilibrium constant for the photodegradation of an aqueous Fluvo solution (1.37×10^{-4} M) exposed to isosbestic monochromatic irradiation at 226 nm, as monitored by HPLC

λ_{isos}/nm	$A_0^{\lambda_{isos}}$	$c_0^{\lambda_{isos}}$/m	$l_{\lambda_{isos}}$/cm	$l_{\lambda_{obs}}$/cm	C_A(pss)/M	C_B(pss)/M	$P_{\lambda_{isos}}$/einstein s^{-1} dm^{-3}	$k^{\lambda_{isos}}_{A\rightleftharpoons B}/s^{-1}$	$K^{\lambda_{isos}}_{A\rightleftharpoons B}$
226	2.41	1.37×10^{-4}	1	1	4.07×10^{-5}	9.59×10^{-5}	1.88×10^{-6}	3.83×10^{-4}	2.35

trum as it is the case for non-conjugated oximes, with the long wavelength absorption transition having a $\pi \rightarrow \pi^*$ character.[27] When exposed to monochromatic irradiation within that region, the spectrum of the solution decreases in the regions 200–215 nm and 226–285 nm and increases in the alternate regions of 215–226 nm and 285–320 nm (Fig. 1). The clearly defined isosbestic points (at 215, 226 and 285 nm) and the smooth evolution of the spectra indicate that the photoreaction is quantitative and proceeds without by-products. Furthermore, *E*-Fluvo and its photoproduct (*Z*-Fluvo, Scheme 1) share a similar overall spectral shape with a 40% maximum variation in absorbance observed at *ca.* 245 nm.

3.3 Determination of the equilibrium constant at an isosbestic irradiation $\left(K^{\lambda_{isos}}_{\rightleftharpoons}\right)$

An *E*-Fluvo aqueous solution was subjected to 226 nm isosbestic/monochromatic irradiation and the photoreaction was monitored by HPLC at various time intervals until the pss was reached. The concentration profiles of *E*- and *Z*-Fluvo were readily fitted by eqn (7) and (8) (Fig. 2), and the fitting parameter, the rate-constant $k^{\lambda_{isos}}_{A\rightleftharpoons B}$, as well as the pss concentrations of the reactive species were determined. Subsequently, the forward (eqn (10)) and reverse (eqn (11)) quantum yield values as well as the equilibrium constant $K^{\lambda_{isos}}_{A\rightleftharpoons B}$ (eqn (12)), could be calculated (Table 1). At λ_{isos} = 226 nm, the initial *E*-isomer is found to be more than twice as photoefficient as its counterpart, as indicated by the value of $K^{\lambda_{isos}}_{\rightleftharpoons}$, which resulted, given that $\varepsilon_A^{\lambda_{isos}} = \varepsilon_B^{\lambda_{isos}}$, in a higher proportion of the *Z*-isomer in the pss composition, as it is usually observed for *trans–cis* photoisomerization.[28,29]

3.4 Recovery of the *Z*-isomer's absorption spectrum

Based on eqn (13), the spectrum of the medium at pss and the spectrum of the *E*-isomer, the electronic absorption spectrum (as absorption coefficients' values) of the *Z*-isomer can be fully reconstructed (Fig. 3).

3.5 Isomers' quantum yields at non-isosbestic irradiation wavelengths

Once the absorption spectrum of the *Z*-isomer was known, the two remaining system unknowns ($\Phi^{\lambda_{irr}}_{A\rightarrow B}$ and $\Phi^{\lambda_{irr}}_{B\rightarrow A}$) could then be calculated for any irradiation wavelength using the quantum yield expressions given by eqn (14) and (15).

Seven monochromatic irradiation wavelengths (λ_{irr} = 290, 285, 280, 270, 260, 245, and 226 nm) that span the isomers' absorption spectra, were selected in this study. The kinetic traces were recorded at a unique observation wavelength λ_{obs} = 245 nm, that corresponds to the most extensive variation of

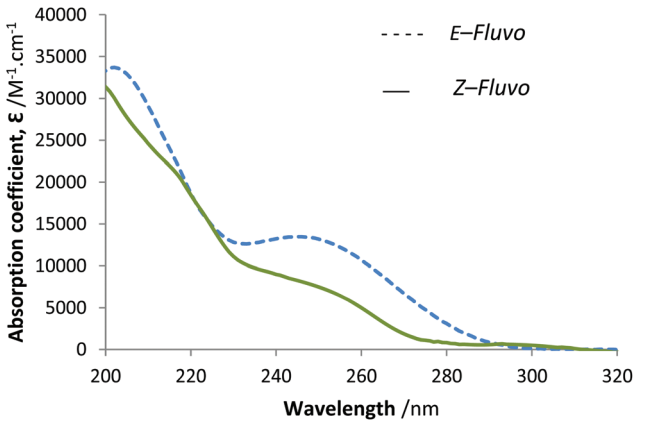

Fig. 3 Electronic absorption spectra (absorption coefficient units) of *E*-(native) and *Z*-Fluvo (recovered).

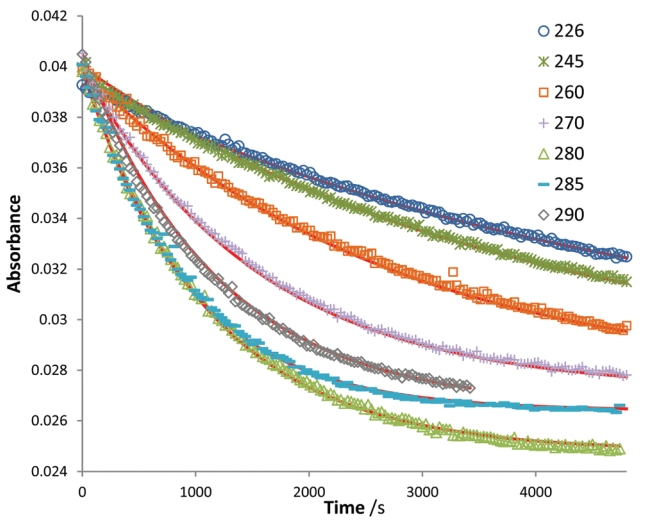

Fig. 4 The photokinetic traces of Fluvo photodegradation in water (2.95×10^{-6} M) at λ_{irr} = 226, 245, 260, 270, 280, 285 and 290 nm and observed at λ_{obs} = 245 nm. The geometric shapes represent the experimental data while the continuous lines represent the model fitted traces using the appropriate model equation.

the absorbance (Fig. 1 and 3). In general, a smooth decrease in absorption over irradiation time was observed eventually reaching a plateau region (Fig. 4), as suggested by HPLC measurements. This represents a typical behaviour of AB(2Φ) systems, which in turn corroborates the mechanism of Fluvo photodegradation (Scheme 1). This is also confirmed by the good

Table 2 Quantum yields, overall rate-constant, absorption coefficient and initial velocity values for Fluvo photodegradation reactions under various monochromatic irradiation wavelengths, as determined by the Φ-order kinetics

λ_{irr}/nm	$A^{\lambda_{irr}/245}_{Fluvo}(0)$	$P_{\lambda_{irr}}$/einstein s^{-1} dm^{-3}	$A^{\lambda_{irr}}$(pss)	$k^{\lambda_{irr}}_{A\rightleftharpoons B}/s^{-1}$	$v^{\lambda_{irr}/\lambda_{abs}}_{0(mod.)}/s^{-1}$	$\varepsilon^{\lambda_{ISOS}}_{A}/M^{-1}$ cm^{-1}	$\varepsilon^{\lambda_{ISOS}}_{B}/M^{-1}$ cm^{-1}	$F^{\lambda_{irr}}(0)$	$\Phi^{\lambda_{irr}}_{A\rightarrow B}$	$\Phi^{\lambda_{irr}}_{B\rightarrow A}$
226	0.0393	6.09×10^{-7}	0.0420	0.000197	-2.20×10^{-6}	14 254	13 802	2.086	0.00383 ± 0.00003	0.00157 ± 0.00027
245	0.0399	5.86×10^{-7}	0.0281	0.000268	-3.09×10^{-6}	13 478	8273	2.095	0.00612 ± 0.00042	0.0038 ± 0.001331
260	0.0398	4.60×10^{-7}	0.0191	0.000380	-4.56×10^{-6}	10 687	4997	2.14	0.0128 ± 0.00064	0.0085 ± 0.00096
270	0.0405	5.21×10^{-7}	0.0109	0.000670	-8.31×10^{-6}	6679	1859	2.19	0.0361 ± 0.00195	0.025 ± 0.0035
280	0.0398	5.51×10^{-7}	0.0031	0.000875	-1.28×10^{-5}	3109	829	2.25	0.0931 ± 0.00275	0.0535 ± 0.0127
285	0.0400	4.70×10^{-7}	0.0031	0.00048	-1.32×10^{-5}	1774	586	2.27	0.2167 ± 0.0059	0.0844 ± 0.0075
290	0.0402	2.56×10^{-7}	0.0028	0.00152	-6.69×10^{-6}	859	596	2.28	0.4349 ± 0.0205	0.0573 ± 0.0184

fitting of the kinetic traces with the model equation, eqn (2), for all non-isosbestic irradiations. Therefore, Fluvo photoconversion obeys Φ-order kinetics.

The kinetic parameters determined for Fluvo photodegradation (Table 2), indicate that the overall rate-constant of photoreaction increases with increasing irradiation wavelength (Table 2). However, as has been comprehensively discussed in previous studies,[10–12] $k^{\lambda_{irr}}_{Fluvo}$ dependence on a number of experimental parameters (eqn (3)), such as initial concentration and irradiation intensity, reduces its ability to inform about the intrinsic photoreactivity of the molecule. Therefore, it is mandatory to define, in subsequent steps, the absolute values of the photoreaction quantum yields at the selected wavelengths.

The recommended hypothesis for this type of studies is that the quantum yields of drugs should *a priori* be supposed to be wavelength dependent and then the hypothesis should be tested experimentally.

It is clearly shown from the results of Table 2 that the forward quantum yield $\left(\Phi^{\lambda_{irr}}_{A\rightarrow B}\right)$ increases with increasing wavelength and is always higher than the reverse quantum yield $\left(\Phi^{\lambda_{irr}}_{B\rightarrow A}\right)$. The most pronounced variation of the quantum yield ratios $(1.4 > \Phi^{\lambda_{irr}}_{A\rightarrow B}/\Phi^{\lambda_{irr}}_{B\rightarrow A} > 7.6)$ is situated in the longest wavelength, 280 to 290 nm, region (ranging between 1.7 and 7.5), whereas, a much more modest change in its values is observed in the region 245–280 nm $(1.4 > \Phi^{\lambda_{irr}}_{A\rightarrow B}/\Phi^{\lambda_{irr}}_{B\rightarrow A} > 1.7)$. Furthermore, the evolution of the forward quantum yield values with wavelength has a defined sigmoid pattern (eqn (16), Fig. 5).

$$\Phi^{\lambda_{irr}}_{A\rightarrow B} = \frac{1}{0.07 + 400 \times e^{-(0.13\times(\lambda_{irr}-250))}} \quad (16)$$

This advantageously enables the determination of *E*-Fluvo quantum yield at any desired wavelength using the sigmoid equation (eqn (16)).

The reverse quantum yield, on the other hand, follows a lower pattern with irradiation wavelength (Fig. 5), with a 5.4-fold maximum span of variation for the recorded set of values (whereas 11.4 was recorded for the forward quantum yield).

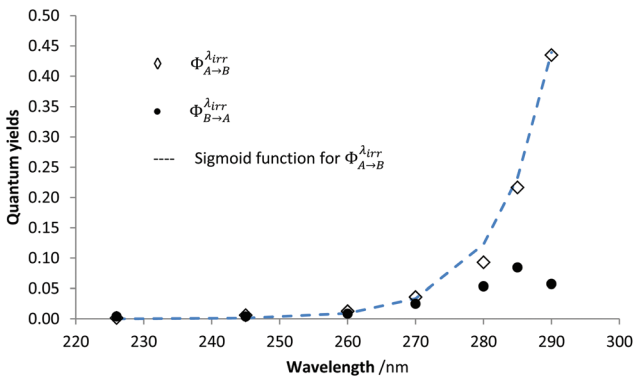

Fig. 5 Average forward $\left(\Phi^{\lambda_{irr}}_{A\rightarrow B}\right)$ (diamonds) and reverse $\left(\Phi^{\lambda_{irr}}_{B\rightarrow A}\right)$ (plain circles) Fluvo quantum yields for irradiation wavelengths 226, 245, 260, 270, 280, 285 and 290 nm.

A similar behaviour has been observed for Montelukast.[12] The differing magnitude of photo-efficiencies between *E*- and its *Z*-Fluvo isomer might suggest a difference in the excited-state associated with each species. The more pronounced difference between the isomers' quantum yields that were recorded in the longest wavelength region indicates that the excited-sate of lowest energy is much more efficient for *E*- than for *Z*-Fluvo. This finding might suppose a more important contribution of the n→π* excited-state in Fluvo phototransformation. In any case, the increase of quantum yields with irradiation wavelengths, observed for a number of drugs studied in our team, does not have at present a full/comprehensive interpretation. Overall, such results may illustrate a case where not only the chemical nature, the geometry of the molecule but also the irradiation conditions impact the photochemical behaviour of the drugs.

The oxime group within *E*-Fluvo is found to be twice as photochemically efficient as the ethene bond in the stilbene-like Montelukast $\left(\Phi^{\lambda_{irr}}_{A\rightarrow B} = 0.012 - 0.18\right)$.[12] In both these cases, as well as for nifedipine,[10] the results show a trend of higher forward quantum yield values for lower-energy excited-states.

In terms of photostability, photoreversibility has the advantage of limiting the depletion of the initial active ingredient to the amounts recorded at the pss, however, the pss concentration (*Z*/*E*) ratios for Fluvo isomers, $C^{\lambda_{irr}}_{B}(\text{pss})/C^{\lambda_{irr}}_{A}(\text{pss}) = \left(\Phi^{\lambda_{irr}}_{A\rightarrow B} \times \varepsilon^{\lambda_{irr}}_{A}\right)/\left(\Phi^{\lambda_{irr}}_{B\rightarrow A} \times \varepsilon^{\lambda_{irr}}_{B}\right)$, increase with wavelength from 2.5 and reach a value of 11.3 at 290 nm, which indicates a substantial degradation of the initial species (*E*-Fluvo). In the case of Fluvo, this represents a significant decrease in dosage as *Z*-Fluvo is biologically inactive,[20] but could be a major issue if for other drugs the photoproduct is toxic. These results stress on the usefulness and necessity of a full kinetics elucidation of drug photodegradation. They also confirm that reliable conclusions about the photoreactivity of a compound can only be reached when using monochromatic irradiation coupled to a treatment using the *Φ*-order kinetics. It is then reasonable to suggest that the ICH recommendations would benefit from introducing an element of photostability assessment of the drugs at low concentration in solution. Such data would not only shed light on the photokinetic behaviour and photodegradation parameters of the drug *in vitro* but also may lay down a platform for an understanding of the behaviour of drugs *in vivo*. Indeed, the distribution of the administered drugs in the skin and eyes of the patients occurs mostly at low concentrations within biological fluids and tissues.[3,4] Many studies have shown that both topical and systemic drugs can cause different conditions including photosensitivity and dermatoses in all-age patients including newborns.[30–33] Even though an exact number of the drugs concerned has not yet been made available, it is nonetheless possible that a very high proportion of existing and future organic drugs, assuming a conservative hypothesis, absorb in the UVA–UVB ranges (some in the visible).[3,4] These types of radiation traverse through the skin with UVA wavelengths penetrating deep into the dermis.[3,4,20] Hence, most of the drugs can reach the excited-state from which they can potentially subsequently photoreact both *in vitro* and *in vivo*. It has been shown that despite the absorption spectrum of Fluvo ends *ca.* 290 nm (Fig. 3), exposing the solution of this drug to UVA–visible light (simulating day light) also caused its degradation.[21] As for most drugs, the variability/progress of the photodegradation depends also on the intensity of the light and/or the duration of the exposure. In this context, the FDA, EMEA and ICH have issued guidelines on the evaluation of the photosafety of all new systemic and topical pharmaceuticals capable of absorbing within the UVB, UVA or visible regions with absorption coefficients above 1000 M^{-1} cm^{-1} as well as existing drugs when unaddressed photosafety concerns arise.[34–36] The regulatory authorities and pharmaceutical industries increasingly recognise photo-induced reactions of pharmaceutical and cosmetic drugs.[3,4,37] In addition, the advent of an ever wide spreading range of phototherapy treatments (including home phototherapy),[38,39] calls for clearer and tighter recommendations for photosafety testing. In this context, testing low concentrated solutions of drugs *in vitro* may arguably benefit the evaluation of the potential and extent of photodegradation that might be undergone by the drug in similar situations *in vivo*. The low concentration studies are also important because the equations of the *Φ*-order kinetics (eqn (3)) show that the rate of photodegradation of drugs increases with decreasing concentration.[10] Such low drug concentrations would mimic *in vivo* conditions as for the latter a maximum substrate concentration was set at 100 μg ml^{-1}, in addition to a recommendation to perform several dilutions during the testing procedure.[36] This is justified by the fact that most drugs reach the circulation, body tissues and eyes in significantly smaller amounts than the original given dose. Furthermore, the ICH currently recommends an irradiance dose of approximately 5 J cm^{-2} UVA doses for the *in vitro* 3T3 Neutral Red Uptake phototoxicity test (3T3 NRU PT) to corroborate natural irradiation conditions comparable to those obtained during prolonged outdoor activities on summer days around noon time, in temperate zones and at sea levels.[36]

Therefore, the conditions of the present study reflect well the situation of drugs in the body as small concentrations (*ca.* 1.3 μg ml^{-1}) and low radiation power (1–2 J h^{-1} cm^{-2}) are employed. Such studies might be thought of as a relevant initial platform, that provide reliable data and valuable information about the inherent photoreactivity of a molecule in solution, to feed the evaluation of drug photosafety and photodegradation *in vivo*.

3.6 Photostabilisation of Fluvo photodegradation using excipient-dyes

There is an evident lack in the literature of useful methods to quantify photostabilisation of drugs. The Q1b document[7] does not propose any detailed procedures in this respect including the case of solutions. In this section, the photoprotection of Fluvo with excipient dyes was assessed by *Φ*-order kinetics.

For this purpose, the UV-absorbing food additive/excipient-dye TRZ was selected as its spectrum overlaps that of Fluvo,

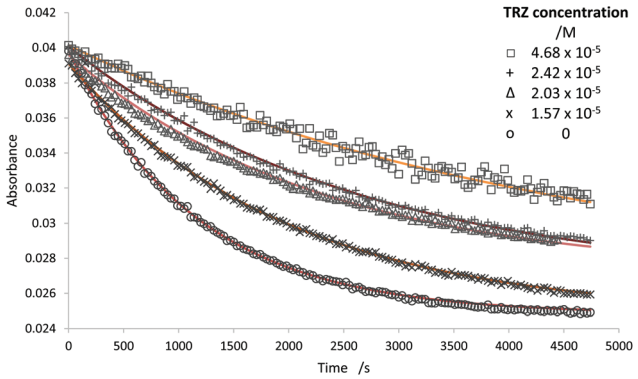

Fig. 6 Effect of increasing TRZ concentrations on the photodegradation traces of 2.95×10^{-6} M aqueous Fluvo solutions when irradiated at 280 nm and observed at 245 nm.

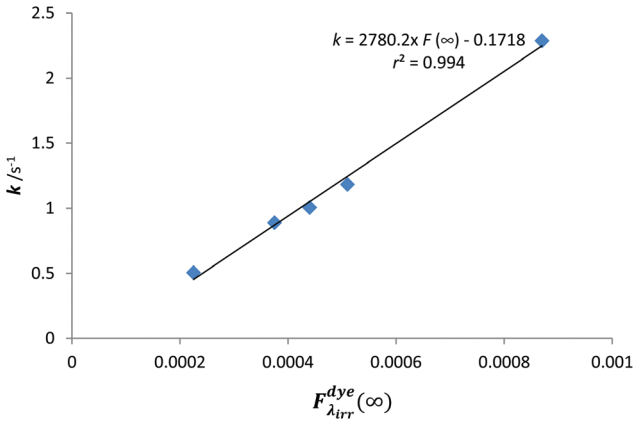

Fig. 7 Linear relationship between Fluvo overall rate-constant of photodegradation in the presence of increasing concentrations of TRZ and the corresponding photokinetic factors $\left(F^{dye}_{\lambda_{irr}}(\infty)\right)$.

Table 3 Dye absorbances, overall reaction rate-constants, photokinetic factors, and percentage reduction in reaction rates of Fluvo photodegradation in the presence of various concentrations of TRZ when irradiated at 280 nm and observed at 245 nm

	$A^{\lambda_{irr}}_{dye}$ [a]	$F^{dye}_{\lambda_{irr}}(\infty)$	$k^{\lambda_{irr}}_{Fluvo}/s^{-1}$	$\frac{k^{\lambda_{irr}}_{Fluvo}\left(A^{\lambda_{irr}}_{dye}=0\right)}{k^{\lambda_{irr}}_{Fluvo}\left(A^{\lambda_{irr}}_{dye}\neq 0\right)}$	% Reduction[b]
Fluvo[c,d]	0	2.28	0.00087	1	0
Tartrazine	0.314	1.18	0.00051	1.71	41.4
(TRZ)	0.406	1.01	0.00044	1.98	49.4
	0.483	0.89	0.00037	2.32	56.9
	0.933	0.51	0.00022	3.87	74.1

[a] Absorbance of the dye measured at the irradiation wavelength of 280 nm for concentrations given in Fig. 6. [b] The constant concentration of Fluvo was 2.95×10^{-6} M. [c] The radiant power value for the experiments was $P_{390} = 5.06 \times 10^{-6}$–$5.18 \times 10^{-6}$ einstein dm^{-3} s^{-1}. [d] The optical path lengths: $l_{\lambda_{irr}} = 2$ cm; $l_{\lambda_{obs}} = 1$ cm.

hence acting as an absorption competitor. Its effect was evaluated on solutions of TRZ of various concentrations, which were each irradiated after the addition of the same amount of Fluvo. It is worth mentioning that prior to the addition of Fluvo, the TRZ solution was considered for the blank experiment on the UV/Vis diode array spectrophotometer. Under these conditions, the temporal evolution of the absorbance of the medium could be recorded without the spectral interference of the dye (the latter however does absorb part of the excitation light).

The resulting kinetic traces ($\lambda_{irr}/\lambda_{obs}$ = 280/245) were fitted with eqn (2) (Fig. 6) and their respective reaction rate-constants were determined (Table 3). Indeed, eqn (1)–(6) apply except that the total absorbance of the medium at the irradiation wavelength in eqn (4) must take into account the presence of the third molecule of the light-absorption competitor, *i.e.* the actual photokinetic factor, $F^{E/Z,\,TRZ}_{\lambda_{irr}}(\infty) = F^{dye}_{\lambda_{irr}}(\infty)$, which involves $A^{\lambda_{irr}/\lambda_{irr}}_{tot}(\infty) = A^{\lambda_{irr}/\lambda_{irr}}_{E/Z}(\infty) + A^{\lambda_{irr}/\lambda_{irr}}_{TRZ}$. The model equation (eqn (2)) fitted all the curves well irrespective of the concentration of TRZ present in solution (though below the limit of its linearity range). Accordingly, the overall photoreaction rate-constant decreased with increasing TRZ concentration. Up to 75% photostabilization of Fluvo was recorded for the highest TRZ concentration used in this study (4.68×10^{-5} M, Table 3). This confirms that the presence of the excipient-dye does not alter the photodegradation pattern and or quantum yields of the photoreactions but only reduces the rate of photodegradation. As stipulated by eqn (4), the photodegradation rate reduction is solely related to a reduction in the value of the photokinetic factor $\left(F^{dye}_{\lambda_{irr}}(\infty)\right)$ which itself is due to an effective increase of the medium absorbance at λ_{irr} $\left(A^{\lambda_{irr}/\lambda_{irr}}_{E/Z}(\infty) + A^{\lambda_{irr}/\lambda_{irr}}_{TRZ}\right)$.

Furthermore, as predicted by eqn (3), a good linear relationship was found between $k^{\lambda_{irr}}_{A\rightleftharpoons B}$ and $F^{dye}_{\lambda_{irr}}(\infty)$ (with the intercept close to zero and a correlation coefficient close to unity) (Fig. 7). A similar phenomenon should also be expected to occur for an increase of the initial concentration of the mother compound (eqn (3)), and hence, the rate of the reaction is concentration-dependent. This confirms that zero- and first-order reaction treatments and interpretation of photodegradation kinetics are neither suitable nor reliable approaches.

The present Φ-order kinetic equations offer however an easy and useful tool to evaluate photostabilisation of drugs in solution.

3.7 Fluvo-actinometer

An additional interesting and useful aspect offered by the equations of Φ-order kinetics is the development of new actinometers. This may represent an important concept because no standard procedures have yet been established for the evaluation of drugs potential for actinometry and/or the proposal of new actinometers.[5,6,40,41] Besides, the ICH adopted quinine hydrochloride actinometer holds a number of drawbacks that raised many questions and doubts about its reliability.[5,6,10,42–44]

The assessment of Fluvo potential for actinometry is set out by preparing solutions of approximately the same concentration and exposing each one to a monochromatic light of given radiant power values selected from a set for each

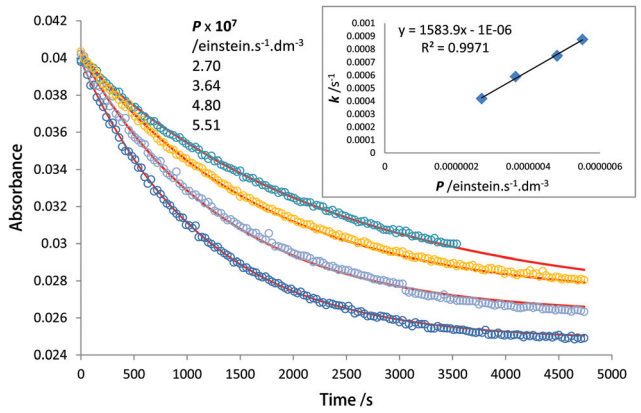

Fig. 8 Effect of increasing the irradiation radiant power ($P_{\lambda_{irr}}$) on the kinetic traces of Fluvo (2.97×10^{-6} M) when irradiated at 280 nm and observed at 245 nm. The circles represent the experimental data while the lines represent the model fitted traces.

irradiation wavelength (260, 270, 280, 285 and 290 nm). The kinetic traces obtained at the observation wavelength of 245 nm were then well fitted to the model eqn (2) (Fig. 8). A linear correlation was observed between the values of $k^{\lambda_{irr}}_{A\rightleftharpoons B}$ and $P_{\lambda_{irr}}$ for each set of irradiation experiments (Table 4) as predicted by eqn (2). Our experimental $\beta_{\lambda_{irr}}$ and $\delta_{\lambda_{irr}}$ values matched well those calculated from eqn (3) and (6).

The gradients of the lines (of $k^{\lambda_{irr}}_{A\rightleftharpoons B}$ *vs.* $P_{\lambda_{irr}}$), the *beta* factors ($\beta_{\lambda_{irr}}$), represent constant coefficients that are independent of the light intensity for each irradiation wavelength. In addition, a linear correlation also exists between $\upsilon^{\lambda_{irr}/\lambda_{obs}}_{0(mod.)}$ and $P_{\lambda_{irr}}$ with gradients specific to each irradiation wavelength defined as the $\delta_{\lambda_{irr}}$ factors (Table 4) as derived from the initial velocity eqn (6). The linear relationships found here confirm the usefulness of Fluvo for actinometry.

Plotting the kinetic parameters $\beta_{\lambda_{irr}}$ and $\delta_{\lambda_{irr}}$ against irradiation wavelengths yields linear correlations within the 260–290 nm irradiation range, as given in Fig. 9.

The procedure for Fluvo-actinometry is set out through two simple strategies for the determination of the radiant power of an unknown source of light $\left(P^{unk.}_{\lambda_{irr}}\right)$ for the range 260–290 nm. Firstly, (a) a fresh solution of *Z*-Fluvo (3×10^{-6} M in water) is subjected to a monochromatic irradiation (λ_{irr}) beam from the unknown source. (b) The experimental kinetic trace hence obtained is fitted to eqn (2) and its $k^{\lambda_{irr}}_{A\rightleftharpoons B}$ value is determined; and/or the $\upsilon^{\lambda_{irr}/\lambda_{obs}}_{0(mod.)}$ of the reaction is derived from the trace (eqn (5)). In the third step, (c) the corresponding values for the $\beta_{\lambda_{irr}}$ and/or $\delta_{\lambda_{irr}}$ factors are worked out from the corresponding relationships at λ_{irr} as given by the equations laid out in Fig. 9. Finally, (d) the unknown radiant power of the source is determined from one of the following equations (eqn (17)).

$$P^{unk.}_{\lambda_{irr}} = \frac{k^{\lambda_{irr}}_{A\rightleftharpoons B}}{\beta_{\lambda_{irr}}} = \frac{\upsilon^{\lambda_{irr}/\lambda_{obs}}_{0}}{\delta_{\lambda_{irr}}} \qquad (17a, b)$$

In order to facilitate the actinometric method even more, the $\upsilon^{\lambda_{irr}/\lambda_{obs}}_{0,\,Cld.}$ values calculated using eqn (6) were compared to those $\left(\upsilon^{\lambda_{irr}/\lambda_{obs}}_{0,\,Exp.}\right)$ obtained as the gradient of the linear fit of the data corresponding to the early stages of the reaction (Fig. 10). A very good agreement has been found, indicating that the initial velocity values can be worked out from the data corresponding to the first 5 to 10 min of Fluvo irradiation. This finding makes the development of AB(2Φ) actinometers a less time-consuming process, which would be decisive for very slow reactions.

Nevertheless, if the concentration or path-lengths used in the unknown light source experiment differ from the ones employed in this study (*i.e.* 2.95×10^{-6} M and $l_{\lambda_{irr}} = 2$ cm, respectively), then $\beta_{\lambda_{irr}}$ must first be adjusted before being substituted in eqn (17a). This can be achieved by dividing the $\beta_{\lambda_{irr}}$ value obtained in step (c) of the procedure above by $2 \times F_{\lambda_{irr}}(pss)$ (the latter corresponding to our experiment) and then multiplying it by the value of the new path-length and the photokinetic factor corresponding to the path-length and concentration used in the unknown light source experiment. Simi-

Table 4 Correlation equations for the variation in the overall rate-constants $\left(k^{\lambda_{irr}}_{Fluvo}\right)$ and initial reaction velocities $\left(\upsilon^{\lambda_{irr}/\lambda_{obs}}_{0}\right)$ with radiant power ($P_{\lambda_{irr}}$) of Fluvo (2.95×10^{-6} M) photodegradation in water ($l_{\lambda_{irr}} = 2$ cm; $l_{\lambda_{obs}} = 1$ cm) together with the corresponding $\beta_{\lambda_{irr}}$ and $\delta_{\lambda_{irr}}$ factors, $F_{\lambda_{irr}}(0)$, $F_{\lambda_{irr}}(pss)$ and the span of radiant power employed for various monochromatic irradiation wavelengths

Irradiation wavelength λ_{irr} /nm	Equation of the line[a]	Correlation coefficient, r^2	$F_{\lambda_{irr}}(0)$	$F_{\lambda_{irr}}(pss)$	$P_{\lambda_{irr}} \times 10^7$/einst s^{-1} dm^{-3}
$k^{\lambda_{irr}}_{Fluvo} = \beta_{\lambda_{irr}} \times P_{\lambda_{irr}} + \text{intercept}$					
260	$818.4 \times P_{260} + 3 \times 10^{-7}$	0.99	2.136	2.199	2.93–4.60
270	$1249 \times P_{270} + 3 \times 10^{-5}$	0.96	2.194	2.244	2.50–5.21
280	$1584 \times P_{280} - 1 \times 10^{-6}$	0.99	2.249	2.277	2.70–5.51
285	$1998 \times P_{285} + 2 \times 10^{-5}$	0.98	2.273	2.287	2.63–4.81
290	$2077 \times P_{290} + 5 \times 10^{-5}$	0.99	2.284	2.291	2.56–4.42
$\upsilon^{\lambda_{irr}/\lambda_{obs}}_{0} = \delta_{\lambda_{irr}} \times P_{\lambda_{irr}} + \text{intercept}$					
260	$-10.58 \times P_{260} + 4.8 \times 10^{-7}$	0.93	2.136	2.199	2.93–4.60
270	$-14.57 \times P_{270} - 8.9 \times 10^{-7}$	0.98	2.194	2.244	2.50–5.21
280	$-25.16 \times P_{280} + 1.3 \times 10^{-6}$	0.99	2.249	2.277	2.70–5.51
285	$-28.11 \times P_{285} + 1.8 \times 10^{-7}$	0.99	2.273	2.287	2.63–4.81
290	$-31.08 \times P_{290} + 1 \times 10^{-6}$	0.99	2.284	2.291	2.56–4.42

[a] $k^{\lambda_{irr}}_{Fluvo}$, $\upsilon^{\lambda_{irr}/\lambda_{obs}}_{0}$ and intercepts expressed in s^{-1}; $\beta_{\lambda_{irr}}$ and $\delta_{\lambda_{irr}}$ in einst^{-1} dm^3.

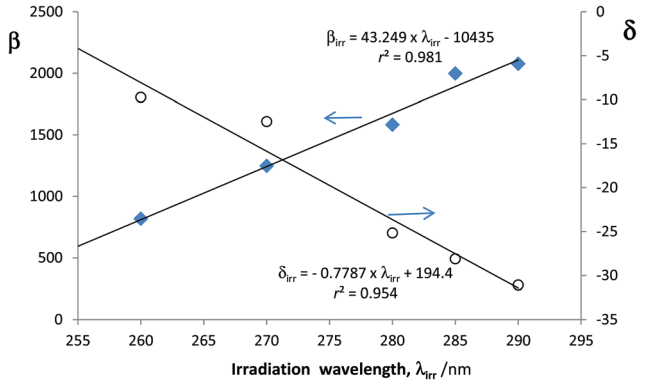

Fig. 9 Linear correlation between $\beta_{\lambda_{irr}}$ and $\delta_{\lambda_{irr}}$ with irradiation wavelength.

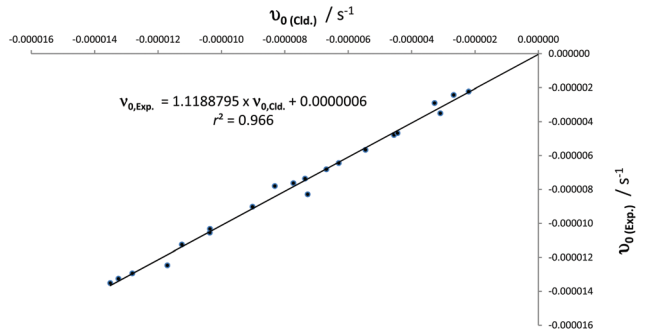

Fig. 10 Correlation between $\nu_{0(\mathrm{Cld.})}^{\lambda_{irr}/\lambda_{obs}}$ and $\nu_{0(\mathrm{Exp.})}^{\lambda_{irr}/\lambda_{obs}}$ for all the sets of Fluvo actinometry experiments in Table 4.

larly, a correction is also needed for $\nu_0^{\lambda_{irr}/\lambda_{obs}}$ if different path-lengths and/or initial concentration are used. This can be achieved by dividing $\nu_0^{\lambda_{irr}/\lambda_{obs}}$ by $2 \times F_{\lambda_{irr}}(0)$ and then multiplying it by the values of the new path-length and the initial photokinetic factor used.

As well as facilitating actinometry studies, $\beta_{\lambda_{irr}}$ can also serve to inform about the photoreaction rate much more reliably than the overall rate-constant or the quantum yields. Unlike $k_{A\rightleftharpoons B}^{\lambda_{irr}}$ and $\Phi^{\lambda_{irr}}$, $\beta_{\lambda_{irr}}$ offers the possibility of comparing the rates of photoreactions within the same or different experimental settings employing the same initial concentrations. This is because $\beta_{\lambda_{irr}}$ takes into account all photoreaction attributes and experimental parameters with the exception of the radiant power (which is hardly replicable between experiments). This parameter is, therefore, an ideal tool for comparing the photoreaction rates between different experiments and we propose to label it as the "*pseudo-rate-constant*". (Similarly, $\delta_{\lambda_{irr}}$ could be considered as the *pseudo-initial velocity* varying only with the terms given in eqn (6) but not with radiant power.) For instance, the wavelength causative range for Fluvo photodegradation is clearly situated above λ_{irr} = 280 nm, with $\beta_{\lambda_{irr}}^{\mathrm{Fluvo}} > 1500$ einst^{-1} dm^3. However, if the wavelength range was overlooked, the photodegradation of Fluvo is 10 to 20 times slower than that of Montelukast with $1.7 \times 10^4 > \beta_{\lambda_{irr}}^{\mathrm{Monte}} > 2.8 \times 10^4$ (despite $\Phi_{A\rightarrow B,\,\mathrm{Fluvo}}^{\lambda_{irr}} > \Phi_{A\rightarrow B,\,\mathrm{Monte}}^{\lambda_{irr}}$).[12] Therefore, this parameter opens new perspectives in comparing photoreaction rates, which have long been awaited, since it is well documented that the (0^{th}-, 1^{st}-, or 2^{nd}-order) overall rate-constant (k) cannot be used comparatively between different experimental settings using the same or different photoreactive species.[5] The quantum yield, on the other hand, informs specifically on the inherent efficiency of a molecule to photoreact in a particular solvent under a given irradiation wavelength, which would be proportional to the reaction rate if and only if the reactive species is the only compound absorbing the excitation light (eqn (3)).[8,10] However, the quantum yield value does not give a full picture on the photoreaction rate if there are more than one species absorbing irradiation in the medium and/or many photochemical steps are involved in the phototransformation mechanism.

4. Conclusion

The above study emphasises the new perspectives offered by the Φ-order kinetic model for photoreversible systems in general. For the particular case of drugs, it sets out a framework for targeted, accurate and complete kinetic studies. Φ-order kinetics then represents a more efficient tool for the assessment and quantification of both photostability and photostabilisation of drugs than the classical treatment based on 0^{th}-, 1^{st}- and 2^{nd}-order kinetics. It can serve in the development of new technological AB(2Φ) devices in photomedicine, targeted drug delivery and photo-responsive drug nano-carrier systems.[45–48] The data provided by such studies may also be of importance for photosafety studies and might be recommended prior to conducting the evermore required *in vivo* safety studies.

Using Fluvo as an example of photoreversible reaction systems, the model (i) fitted its full kinetic traces; (ii) allowed the determination of the overall-rate constant; (iii) offered the pseudo-rate-constant beta factors as new and reliable kinetic parameters truly reflective of the intra- and inter-experiment rate of photoreactions; (iv) allowed the quantification of effects of photostabilising additives; and (v) presented Fluvo as an accurate and reliable actinometer for the 260–290 nm irradiation range.

References

1 J. M. Koheler, In *Drug-Induced Diseases: Prevention*, detection and management, ed. J. E. Tisdale and D. A. Miller, Hearthside Publishing, Bethesda, 2010, pp. 117–134.
2 E. Bjertness, *Solar Radiation and Human Health*, The Norwegian Academy of Science and Letters, Oslo, 2008, pp. 102–113.
3 J. Ferguson, Investigation of drug-induced photosensitivity in man, *Toxicology*, 2006, **226**, 25–26.

4 J. Ferguson, Photodermatology, in *Photodermatology*, ed. J. Ferguson and J. S. Dover, Manon Publishing Ltd, London, 2006.
5 J. T. Piechocki and K. Thoma, *Pharmaceutical Photostability and Photostabilisation Technology*, Informa Healthcare, London, 2010.
6 H. H. Tonnesen, *Photostability of Drugs and Drug Formulations*, CRC Press, London, 2nd edn, 2004.
7 ICH, Guidance for industry Q1B photostability testing of new drug substances and products, *Fed. Regist.*, 1996, **62**, 27115–27112.
8 M. Maafi and R. G. Brown, The kinetic model for AB(1Φ) systems: A closed-form integration of the differential equation with a variable photokinetic factor, *J. Photochem. Photobiol., A*, 2007, **187**, 319–324.
9 M. Maafi and R. Brown, Kinetic analysis and kinetic elucidation options for AB(1k,2Φ) systems. New Spectrokinetic methods for photochromes, *Photochem. Photobiol. Sci.*, 2008, **7**, 1360–1372.
10 W. Maafi and M. Maafi, Modelling Nifedipine Photodegradation, Photostability and Actinometric Properties, *Int. J. Pharm.*, 2013, **456**, 153–164.
11 M. Maafi and W. Maafi, Φ-order kinetics of photoreversible drug reactions, *Int. J. Pharm.*, 2014, **471**, 536–543.
12 M. Maafi and W. Maafi, Montelukast photodegradation: Elucidation of Φ-order kinetics, determination of quantum yields and application to actinometry, *Int. J. Pharm.*, 2014, **471**, 544–552.
13 N. Fukui, Y. Suzuki, T. Sugai, J. Watanabe, S. Ono, N. Tsuneyama and T. Someya, Promoter variation in the catechol-*O*-methyltransferase gene is associated with remission of symptoms during fluvoxamine treatment for major depression, *Psychiatry Res.*, 2014, **218**, 353–355.
14 D. P. Figgitt and K. J. McClellan, Fluvoxamine: An updated review of its use in the management of adults with anxiety disorders, *Drugs*, 2000, **60**, 925–954.
15 P. Benfield and A. Ward, Fluvoxamine: a review of its pharmacodynamics and pharmacokinetic properties, and therapeutic efficacy in depression illness, *Drugs*, 1986, **32**, 313–334.
16 M. Honda, K. Uchida, M. Tanabe and H. Ono, Fluvoxamine, a selective serotonin reuptake inhibitor, exerts its antiallodynic effects on neuropathic pain in mice via 5-HT2A/2C receptors, *Neuropharmacology*, 2006, **51**, 866–872.
17 A. Velasco, C. Alamo, J. Heras and A. Carvajal, Effects of fluoxetine hydrochloride and fluvoxamine maleate on different preparations of isolated guinea-pig and rat organ-tissues, *Gen. Pharmacol.*, 1997, **28**, 509–512.
18 D. Muck-Seler, N. Pivac and M. Diksic, Acute treatment with fluvoxamine elevates rat brain serotonin synthesis in some terminal regions: an autoradiographic study, *Nucl. Med. Biol.*, 2012, **39**, 1053–1057.
19 H. A. Panahia, Y. T. E. Monirib and E. Keshmirizadeh, Synthesis and characterization of poly[*N*-isopropylacrylamide-*co*-1-(*N*,*N*-*bis*-carboxymethyl)amino-3-allylglycerol] grafted to magnetic nano-particles for the extraction and determination of fluvoxamine in biological and pharmaceutical samples, *J. Chromatogr., A*, 2014, **1345**, 37–42.
20 G. Miolo, S. Caffieri, L. Levorato, M. Imbesi, P. Giusti, T. Uz, R. Manev and H. Manev, Photoisomerization of fluvoxamine generates an isomer that has reduced activity on the 5-hydroxytryptamine transporter and does not affect cell proliferation, *Eur. J. Pharmacol.*, 2002, **450**, 223–229.
21 J. W. Kwon and K. L. Armbrust, Photo-isomerization of fluvoxamine in aqueous solutions, *J. Pharm. Biomed. Anal.*, 2005, **37**, 643–648.
22 K. Iijima, M. Suzuki, T. Sakaizumi and O. Ohashi, Molecular structure of gaseous acetoxime determined by electron diffraction, *J. Mol. Struct.*, 1997, **413–414**, 327–331.
23 M. Black and K. Armbrust, Final Report: The Environmental Occurrence, Fate, and Ecotoxicity of Selective Serotonin Reuptake Inhibitors (SSRIs) in Aquatic Environments, 2007. Available at: http://cfpub.epa.gov/ncer_abstracts/index.cfm/fuseaction/display.abstractDetail/abstract/1755/report/F, accessed on 3 January 2015.
24 M. Maafi, The potential of AB(1Φ) systems for direct actinometry. Diarylethenes as successful actinometers for the visible range, *Phys. Chem. Chem. Phys.*, 2010, **12**, 13248–13254.
25 M. Maafi and R. Brown, General analytical solutions for the kinetics of AB(k,Φ) and ABC(k,Φ) systems, *Int. J. Chem. Kinet.*, 2005, **37**, 162–174.
26 M. Maafi and R. Brown, Analysis of diarylnaphthopyran kinetics. Degeneracy of the kinetic solution, *Int. J. Chem. Kinet.*, 2005, **37**, 717–727.
27 A. Gilbert and J. Bagott, *Essentials of molecular photochemistry*, Blackwell Science, Oxford, 1991.
28 D. C. Neckers, D. H. Volman and G. Von Bunau, *Advances in photochemistry*, John Wiley & Sons, New York, 1995, vol. 19.
29 J. Singh, *Photochemistry and pericyclic reactions*, New Age International, New Delhi, 2005.
30 Z. Kutlubay, A. Sevim, B. Engin and Y. Tuzun, Photodermatoses, including phototoxic and photoallergic reactions (internal and external), *Clin. Dermatol.*, 2004, **32**, 73–79.
31 A. Arnold, C. Pedroza and E. Tyson, Phototherapy in ELBW newborns: Does it work? Is it safe? The evidence from randomized clinical trials, *Semin. Perinatol.*, 2014, **38**, 452–464.
32 L. Feldmeyer, G. Shojaati, K. S. Spanaus, A. Navarini, B. Theler, D. Donghi, M. Urosevic-Maiwald, M. Glatz, L. Imhof, M. J. Barysch, R. Dummer, M. Roos, L. E. French, C. Surber and G. F. L. Hofbauer, Phototherapy with UVB narrowband, UVA/UVBnb, and UVA1 differentially impacts serum 25-hydroxyvitamin-D3, *J. Am. Acad. Dermatol.*, 2013, **69**, 530–536.
33 A. M. Drucker and A. M. C. F. Rosen, Drug-induced photosensitivity: culprit drugs, management and prevention, *Drug Saf.*, 2011, **34**, 821–837.
34 ICH(S10), ICH Harmonised Tripartite Guideline Photosafety Evaluation of Pharmaceuticals S10, 2013. Available

at: http://www.ich.org/fileadmin/Public_Web_Site/ICH_Products/Guidelines/Safety/S10/S10_Step_4.pdf, accessed on 3 January 2015.

35 FDA Food and Drug Administration Center for Drug Evaluation and Research (CDER). Guidance for Industry: Photosafety Testing, 2003. Available at: http://www.fda.gov/cder/guidance/index.htm, accessed on 3 January 2015.

36 The European Agency for the Evaluation of Medicinal Products (EMEA). Committee for Proprietary Medicinal Products (CPMP). Note for guidance on photosafety testing, 2002. CPMP/SWP/398/01. Available at: http://www.emea.eu.int/, accessed on 3 January 2015.

37 C. Krul, W. Maas, R. Van Meeuwen, N. De Vogel and M. J. Steenwinkel, In vivo photogenotoxicity testing, bridging the gap between in vitro photogenotoxicity and photocarcinogenicity testing, *Toxicology*, 2006, **226**, 1–25.

38 H. Cameron, S. Yule, R. S. Dawe, H. Ibbotson, H. Moseley and J. Ferguson, Review of an established UK home phototherapy service 1998–2011: improving access to a cost-effective treatment for chronic skin disease, *Public Health*, 2014, **128**, 317–324.

39 T. Gambichler, S. Terras and A. Kreuter, Treatment regimens, protocols, dosage, and indications for UVA1 phototherapy: facts and controversies, *Clin. Dermatol.*, 2013, **31**, 438–454.

40 H. J. Kuhn, S. E. Braslavsky and R. Schmidt, Chemical actinometry (IUPAC Technical Report), *Pure Appl. Chem.*, 2004, **76**, 2105–2146.

41 M. Montali, A. Credi, L. Prodi and M. T. Gandolfi, *Handbook of photochemistry*, CRC Press – Taylor & Francis, Boca Raton-London-New York, 3rd edn, 2006.

42 S. W. Baertschi, Commentary on the quinine actinometry system described in the ICH draft guideline on photostability testing of new drug substances and products, *Drug Stab.*, 1997, **1**, 193–195.

43 S. W. Baertschi, K. M. Alsante and H. H. Tonnesen, A critical assessment of the ICH guideline on photostability testing of new drug substances and products (Q1B): recommendation for revision, *J. Pharm. Sci.*, 2010, **99**, 2934–2940.

44 C. A. De Azevedo Filho, D. De Filgueiras Gomes, J. P. De Melo Guedes, R. M. F. Batista and B. S. Santos, Considerations on the quinine actinometry calibration method used in photostability testing of pharmaceuticals, *J. Pharm. Biomed. Anal.*, 2011, **54**, 886–888.

45 B. M. Wohl and J. F. J. Engebersen, Responsive layer-by-layer materials for drug delivery, *J. Controlled Release*, 2012, **158**, 2–14.

46 I. Tomatsu, K. Peng and A. Kros, Photoresponsive hydrogels for biomedical applications, *Adv. Drug Delivery Rev.*, 2011, **63**, 1257–1266.

47 N. Fomina, J. Sankaranarayanan and A. Almutairi, Photochemical mechanisms of light-triggered release from nanocarriers, *Adv. Drug Delivery Rev.*, 2012, **64**, 1005–1020.

48 M. Feliciano, D. Vylta, K. A. Medeiros and J. J. Chambers, The $GABA_A$ receptor as a target for photochromic molecules, *Bioorg. Med. Chem.*, 2010, **18**, 7731–7738.

